Arabian Journal of Chemistry (2022) **15**, 104075

King Saud University

Arabian Journal of Chemistry

www.ksu.edu.sa
www.sciencedirect.com

ORIGINAL ARTICLE

Antimicrobial activities of polyethylene glycol and citric acid coated graphene oxide-NPs synthesized via Hummer's method

Tariq Munir [a], Muhammad Imran [a], Saima Muzammil [b], Abdul Ahad Hussain [c], Muhammad Fakhar-e Alam [a], Arslan Mahmood [a,*], Amjad Sohail [a], Muhammad Atif [d], Sulman Shafeeq [e,*], Muhammad Afzal [f]

[a] *Department of Physics, Government College University Faisalabad (GCUF), Allama Iqbal Road, Faisalabad 38000, Pakistan*
[b] *Departmant of Microbiology, Government College University Faisalabad, Allama Iqbal Road, Faisalabad, Pakistan*
[c] *Department of Physics, University of Agriculture Faisalabad, Faisalabad 38040, Pakistan*
[d] *Department of Physics and Astronomy, College of Science, King Saud University, Riyadh 11541, Saudi Arabia*
[e] *Department of Microbiology, Tumor and Cell Biology, Karolinska Institute, Stockholm, Sweden*
[f] *Departmant of Bioinformatics and Biotechnology, Government College University Faisalabad, Allama Iqbal Road, Faisalabad, Pakistan*

Received 12 April 2022; accepted 22 June 2022
Available online 25 June 2022

KEYWORDS

PEG;
Graphene oxide (GO);
Antimicrobial;
A. hydrophila;
E. coli;
F. avenaceum

Abstract Graphene oxide (GO)-NPs possess excellent physicochemical and biological properties and could have prominent antimicrobial activities. We used solution-based Hummer's method to synthesize pure, CA coated and PEG coated GO-NPs and the XRD revealed hexagonal lattice structure and the crystallite size of pure and coated GO-NPs calculated in the range of 7–16 nm. In addition, a spongy like surface in pure GO-NPs and randomly crumpled like surface by using the CA and PEG coating agents was also identified and SEM images irregular, non-uniform and rod shape morphology of the graphite powder. The GO in the UV region and the band gap decreased from 2.30 to 2.03 eV while different modes (C═C and C═O) on the surface of pure and coated GO-NPs were evident as indicated by Raman spectra. Finally, *in-vitro* antimicrobial activity was assessed against two-gram negative bacterial strains viz. *A. hydrophila*and *E. coli* and one fungal stain *F. avenaceum* at 10 and 20 mg/mL concentrations. Our results indicated enhancement in the inhibition zones of pure GO-NPs from 8 to 17 mm, PEG coated GO-NPs from 8 to 20 mm and CA coated GO-NPs from 8 to 17 mm respectively. Overall the PEG coated

* Corresponding author.
E-mail addresses: arslan4physics@gmail.com (A. Mahmood), sulman.shafeeq@ki.se (S. Shafeeq).
Peer review under responsibility of King Saud University.

Production and hosting by Elsevier

https://doi.org/10.1016/j.arabjc.2022.104075
1878-5352 © 2022 The Authors. Published by Elsevier B.V. on behalf of King Saud University.
This is an open access article under the CC BY license (http://creativecommons.org/licenses/by/4.0/).

GO-NPs had prominent antimicrobial activities and we recommend application of polymer coated GO-NPs for wound healing process.

© 2022 The Authors. Published by Elsevier B.V. on behalf of King Saud University. This is an open access article under the CC BY license (http://creativecommons.org/licenses/by/4.0/).

1. Introduction

The potential threat of bacterial infectious diseases which include Pneumonia, Anthrax, Cholera, Tuberculosis, Botulism, and Tetanus cause of distressing in millions of people. The treatment of pathogenic bacterial infection possible with drugs createsa lot of side effects on human health (Ahmad et al., 2021; Muhammad et al., 2020). These side effects are reduced by using the non-traditional antibacterial nanomaterials (Munir et al., 2021; Munir et al., 2020; Robkhob et al., 2020). The carbon base nanomaterials/ nanosheet (Graphene and graphene oxide) have excellent physicochemical and biological properties and are preferred for biomedical applications which include antibacterial, anticancer, antifungal, antioxidant, and antiviral infections (Bilal et al., 2021; Chung et al., 2013; Priyadarsini et al., 2018). Recent studies are provided detailed information about synthetic, miscible, and biodegradable polymers-coated nanomaterials that improve the stability, biocompatible and nontoxic for cells and tissues (Sunderrajan et al., 2018). The PEG is a hydrophilic polymer and CA is an organic acid that reacts with Graphene oxide nanoparticles (GO-NPs) to increase its physical and chemical characteristics.

Graphene is the most prominent material in lab research and industrial applications (Kamenska et al., 2021). The chemical addition of functional groups (OH, COOH) in graphene materialthen it was changed into graphene oxide. Nowadays, the main challenge for researchers is the synthesis of graphene-based nanomaterials with control physical properties (Al Mogbel et al., 2021). The organic/polymer coating agents increase the agglomeration level in graphene base nanomaterial (Chowdhury et al., 2014). The GO materials show excellent biocompatibility, tissue repair and enhance the proliferation level of stem cells. The GO-NPs have antifungal, anticancer, and antibacterial activities against gram-negative and positive strains of bacteria (Placha and Jampilek, 2019). Likewise, GO-NPs can damage the bacterial membrane and cause oxidative stress the bacteria was dead. A huge number of coating agents were used to enhance antimicrobial activity (Sengupta et al., 2019). Al Mogbel et al (2021) reported that the PVP-coated GO-NPs provided significant results in the field of biophysics but they have weak mechanical properties as compared to GO-NPs. After coating the GO-NPs it was identified that the hydrogen bonding takes place between hydroxyl and carboxylic groups in GO with pyrrolidone rings in PVP. The PVP-coated GO-NPs enhance tissue compatibility, limited absorption of water, and high mechanical strength and could have substantial biological activities.

The linear synthetic Polyethylene glycol (PEG) and biodegradable Citric acid (CA) coated Graphene oxide (GO)-NPs was synthesized by using Hummer's method. The prepared samples were characterized with different techniques like X-ray powder diffraction (XRD), Scanning electron microscope (SEM), Ultraviolet–visible spectroscopy (UV–VIS) and Raman spectroscopy. The bio assay was completed with the help of well diffusion method against two gram negative strains such as *Aeromonas hydrophila* (*A. hydrophila*), *Escherichia coli* (*E. coli*), and one fungi *Fusarium avenaceum* (*F. avenaceum*).

2. Experiment

2.1. Chemicals

To investigate the quantitative analysis of pure and coated GO-NPs were synthesized by using various chemicals such as graphite powder, hydrogen peroxide (H_2O_2), sulphuric acid (H_2SO_4), and potassium permanganate ($KMnO_4$), de-ionize water, citric acid, and polyethylene glycol. The prepared pure and coated GO-NPswere used for antimicrobial activities.

2.2. Synthesis of GO-NPs

Hummer's method was used to synthesize of GO-NPs in which 3 g of graphite powder was dissolved in 75 mL of H_2SO_4. After that, the materials were stored in an ice bath and continuous stirring on a magnetic stirrer for three hours. During this process, the 9 g of $KMnO_4$ was added slowly to the graphite powder solution and the temperature was adjusted at 15 °C to control the reaction rate. Furthermore, the 300 mL of de-ionized water was added dropwise to dilute the solution and then remove from the ice bath to increase the temperature upto 50 °C. In the end, the reaction was terminated by using 15 mL of H_2O_2, and the final product was filtered using filter paper. The materials were dried in an oven at 100 °C for 3 days and the materials were ground by using mortar and pestle.

2.3. Citric acid and Polyethylene glycol coated GO-NPs

During the synthesis process, the 0.5 g polyethylene glycol was added to 10 mL of de-ionized water. The prepared PEG solution was added to the GO solution to obtain the PEG-coated GO materials. After that, the same process was repeated for citric acid 0.2 g to obtain the CA-coated GO materials.

2.4. Material characterization techniques

The prepared pure and coated GO-NPs were characterized by using various characterization techniques such as XRD, SEM, UV–VIS, and Raman spectroscopy. The structural analysis was identified by XRD (Cu-Kα radiation, D8 Advance, Bruker, X'Pert3 MRD XL), and the surface morphology was investigated via SEM (tabletop) and UV–VIS (Lambda 25, Perkin Elmer) was used to identifyabsorbance bands. Finally, confocal Raman spectroscopy (MN STEX_PR1100) was used to calculate the different modes attached to the surface of pure and coated GO-NPs.

2.5. Antimicrobial assay

2.5.1. Culturing of Aeromonas hydrophila, Escherichia coli, and Fusarium avenaceum

The well diffusion method was used to culture bacteria and fungi{*A. hydrophila* (CECT 839), *E. coli* (MTCC 443) and *F. avenaceum* (PDA)}to investigate the antimicrobial activity. The initial step was preferred to solidifying media and then cultured samples were implanted in Petri dishesfor 24 h at 37 °C. After that the different concentrations (10 and 20 mg/mL) of pure, CA coated and PEG coated GO-NPs and then again incubated for 24 h to investigate the changes in the inhibition zone.

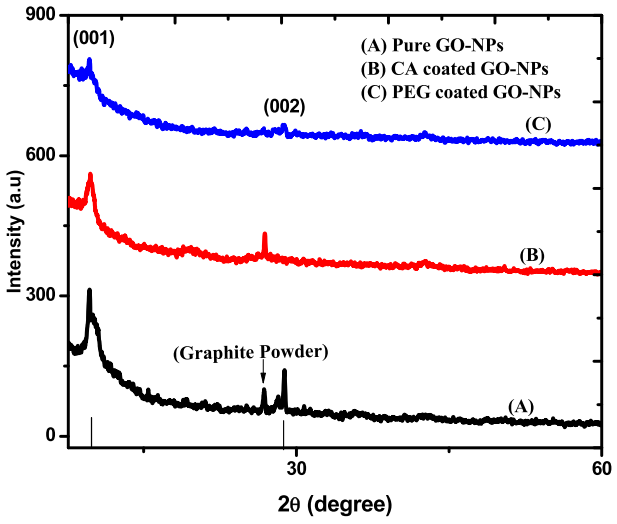

Fig. 1 XRD spectrum of pure and coated GO-NPs.

Table 1 Shows the d-spacing, FWHM and crystallite size of pure and coated GO-NPs.

Nanoparticles	d-spacing Value (nm)	FWHM (001) (rad)	Crystallite size (nm)
Pure GO-NPs	0.9069	0.020	7
CA coated GO-NPs	0.8923	0.019	7.4
PEG coated GO-NPs	0.8926	0.009	15.4

3. Results and discussion

3.1. XRD analysis

The XRD analysis was performed to investigate the crystalline nature of pure and coated GO-NPs. Fig. 1 shows the multiple diffracted peaks representing the different miller indices planes such as (001) and (002) compared with previously published data (Jabbar et al., 2017; Johra et al., 2014). The hexagonal lat-

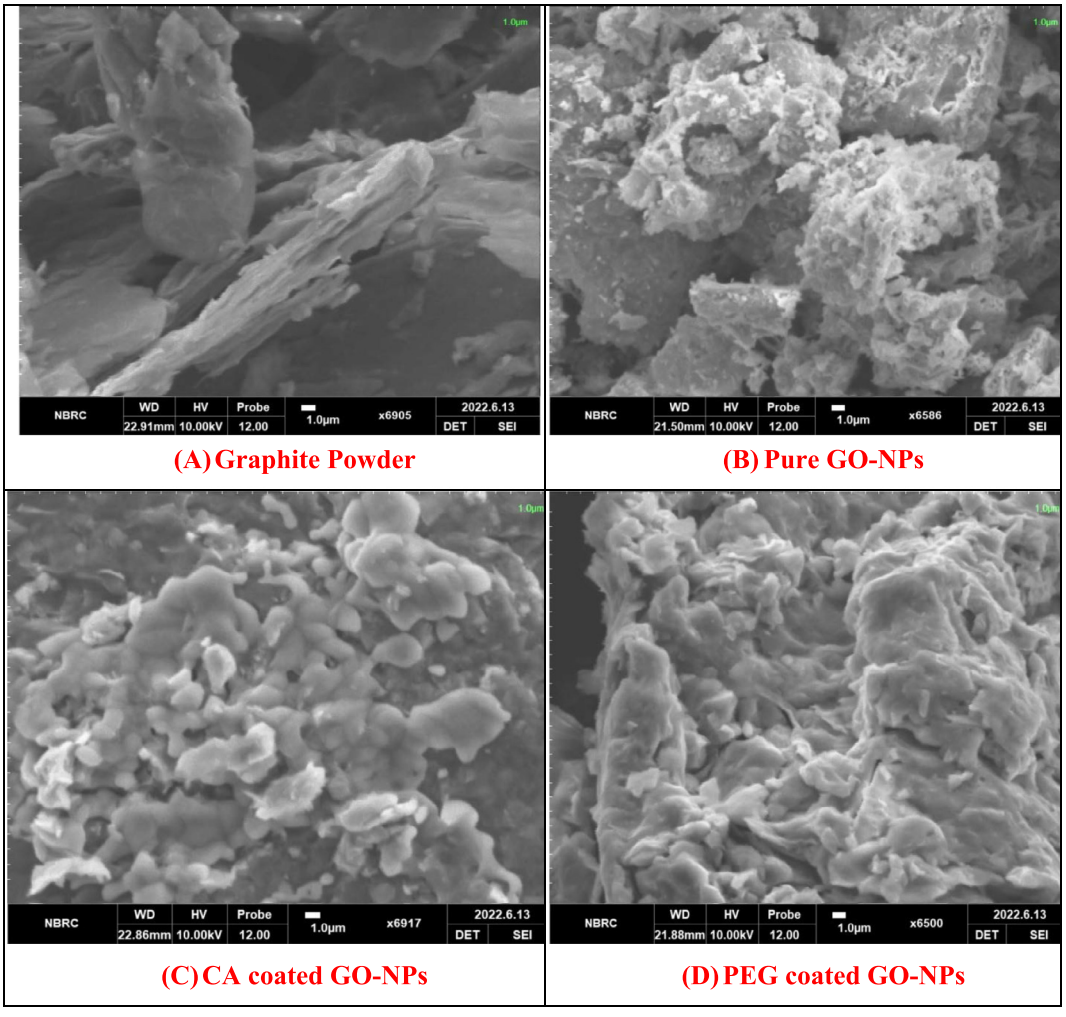

Fig. 2 SEM analysis of Graphite powder, Pure and coated GO-NPs.

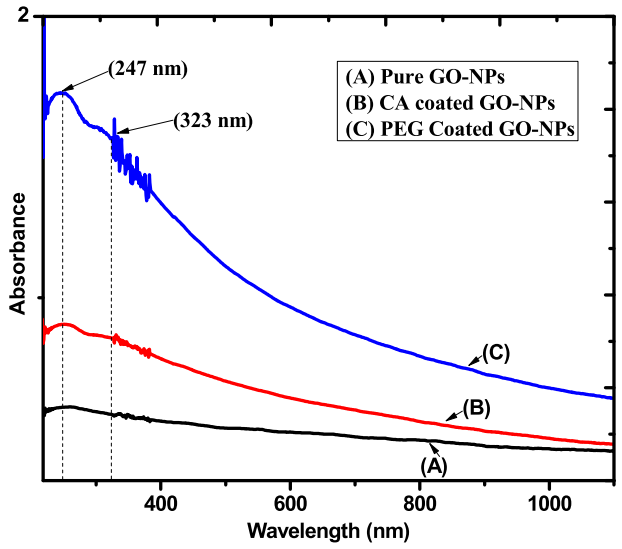

Fig. 3 UV–VIS spectrum of pure and coated GO-NPs.

tice structureidentified the most prominent peaks of pure and coated GO-NPs. The analysis indicated that coating agents enhance the intensity level which depends upon the orientation of the peaks and no extra peak appeared. Moreover, the CA coating agent shifted the peak toward shorter (2θ) as compared to pure and PEG-coated GO-NPs (Jihad et al., 2021). In the case of graphite powder, the d-spacing (0.3395 nm) and crystallite sizeslightly increased as compared to pure and coated GO-NPs. The crystallite size, FWHM, and d-spacing value of pure and coated GO-NPswere calculated by using equations ((1) and (2)). Table 1 indicated that PEG-coated GO-NPscrystallite size is much greater as compared to pure andCA-coated GO-NPs.

$$D = \frac{k\lambda}{\beta \cos\theta} \tag{1}$$

$$a = d_{hkl}\sqrt{h^2 + k^2 + l^2} \tag{2}$$

3.2. SEM analysis

The SEM analysis was used to identify the surface morphology of the pure and coated GO-NPs. Fig. 2 (A) Graphite power (B)

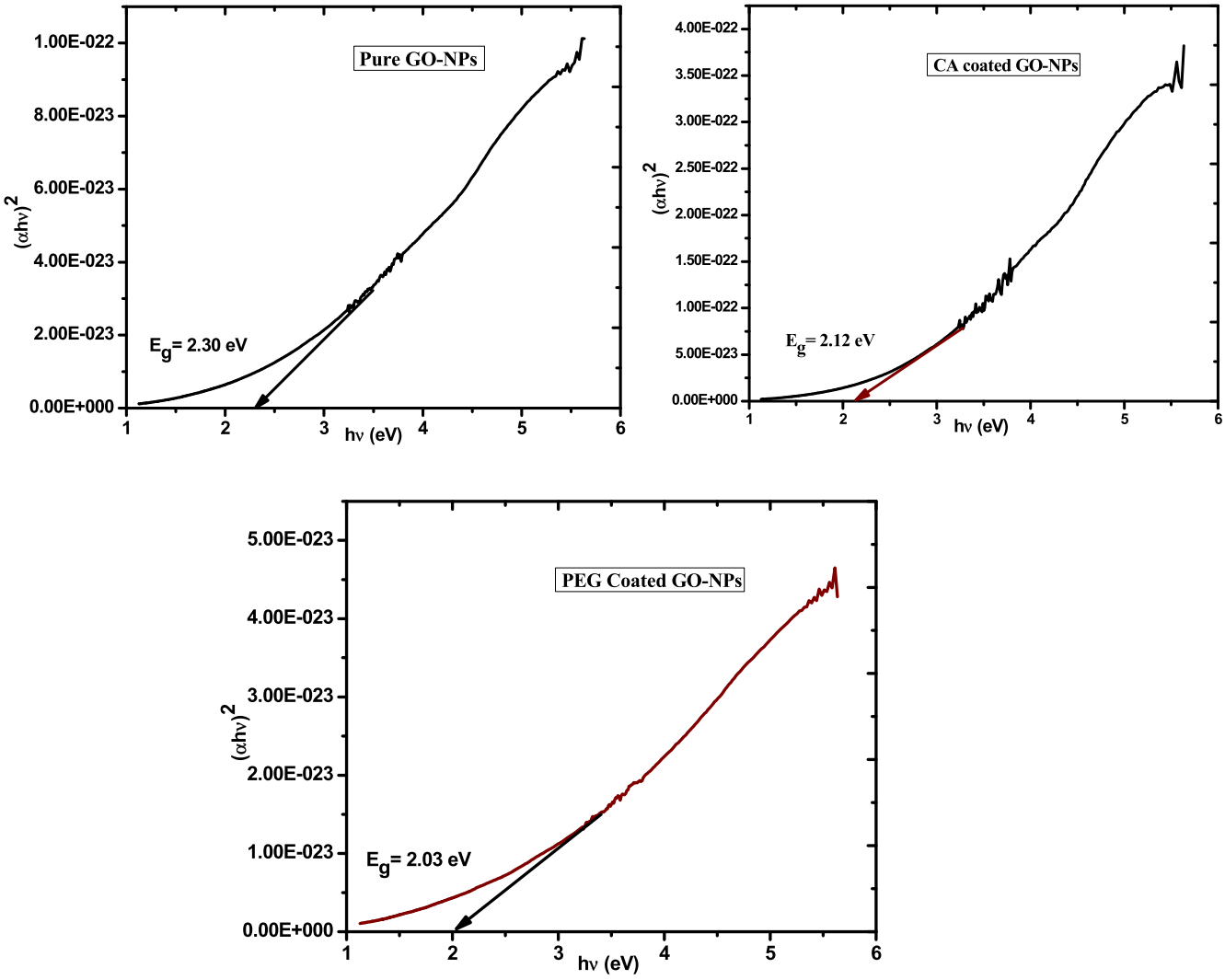

Fig. 4 Band gap of pure and coated GO-NPs.

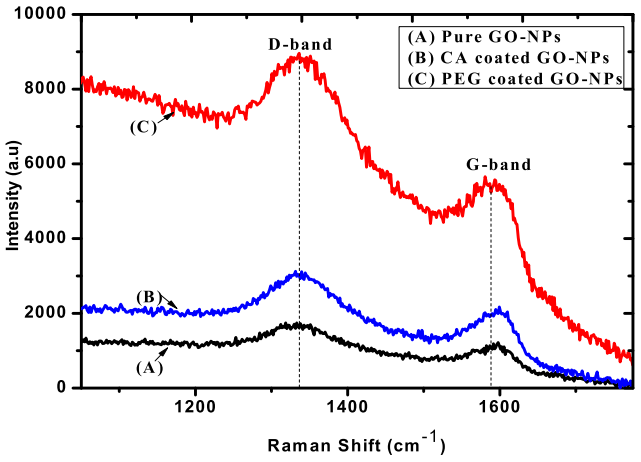

Fig. 5 Raman spectrum of pure and coated GO-NPs.

Pure GO-NPs (C) CA-coated GO-NPs (D) PEG-coated GO-NPs. Fig. 2 (A) shows the irregular, non-uniform, and rod-like shape attachedto the surface of the sheet. Fig. 1(B) represents the wrinkles and spongy-like surface of pure GO-NPs. It means that the GO-NPs have a large surface area due to oxidation as compared to Graphite powder (Samadian et al., 2020; Hayes et al., 2015). Likewise, Fig. 2 (C) indicatesthe surface morphology of GO-NPs changes with CA and also shows that the agglomeration increases between GO-NPs. Fig. 2(D) shows the strong interaction between the PEG and GO-NPs. Due to this interaction, the randomly crumpled-like morphology appeared in PEG-coated GO-nanomaterial.

3.3. UV–VIS analysis

Theoptical absorbance spectrum of pure and coated GO-NPs was investigated via UV–VIS spectroscopy. Fig. 3 indicates the spectrums of pure, CA-coated, and PEG-coated GO-NPs in which the 1st peak at 247 nm and 2nd peak at 323 nm. Furthermore, the coating agents CA and PEG enhance the intensity level of the spectrums (Georgieva et al., 2021). The peaks at 247 nm show the conformation of GO-NPsandit represented the π-π* transition of the C—C bond. Furthermore, the 2nd peak at 323 nm expressed the n-π* transition of the C═O bond (Bhargava and khan, 2018). The Tauc relationexpressed in equation (III) was used to calculatethe band gap of pure, CA-coated, and PEG-coated GO-NPs (Gospodinova et al., 2021). Fig. 4 shows that band gap decreases (2.30–2.01 eV) due toan increase in the particle size of CA-coated and PEG-coated GO-NPs.

$$(\alpha h\nu)1/2 = A(h\nu - Eg) \quad \text{(III)}$$

3.4. Raman spectroscopy analysis

The Raman spectroscopy was used to collect structural information such as disorder, defect, and doping level. Itis an essential tool to provide details informationabout carbon-based nanomaterials. Fig. 5 indicates the spectrum of pure, CA-coated, and PEG-coated GO-NPs which appear in D and G bands (Li et al., 2018). The D band at 1336 cm^{-1} indicate the presence of a C═C ring and the G band that appeared at 1586 cm^{-1} shows that sp^2 hybridization and also expressed the scattering E_{2g} phonon. After coating the GO-NPs were expressed G-band broader due to a reduction in the size of the sp^2 plan which cause the excess oxidation (Orth et al., 2013). The D band was expressed more intense beakswhich means that the more reduction due to coated GO-NPs. Likewise, the intensity level increase of coatedGO-NPs due to surface activity and the relative intensity of D and G indicates the cluster size increase. Furthermore, the previous study provided the detailed information about the intensity level increase at every stage of modification (Usman et al., 2018).

3.5. Antimicrobial assay

Fig. 6 shows that*in-vitro* antimicrobial activity was assessed by using the well diffusion method. The reactive oxygen species was responsible to increase the inhibition zone by using the different doses of pure and coated GO-NPs. The free radical played a central role to damage the cell wall cause the bacteria dead. This study was done with the help of two different concentrations (10 mg/mL and 20 mg/mL) of pure and surface-coated GO-NPs against two gram-negative bacteria such as *Aeromonas hydrophila* and *Escherichia coli*, as well as one filamentous fungi *Fusarium avenaceum* (Olborska et al., 2020; Valentini et al., 2019). The inhibition zone change by using 10 mg/mL of pure, PEG and CA GO-NPs was investigated for *A. hydrophila* (8,8, and 8 mm), *E. coli* (15, 13, and

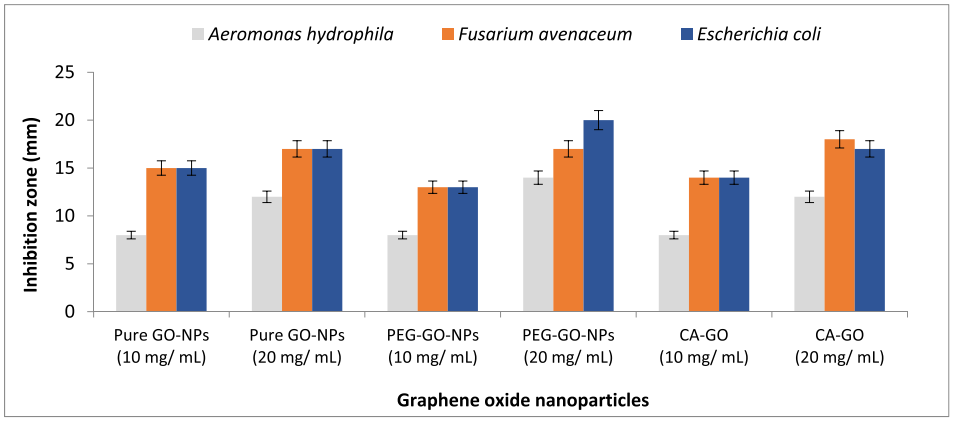

Fig. 6 Antimicrobial activity of pure and coated GO-NPs.

14 mm), and *F. avenaceum* (15, 13, and 14 mm). Furthermore, by increasing the concentration upto 20 mg/mL then inhibition zone change was investigated for*A. hydrophila* (12, 14, and 12 mm), *E. coli* (17, 20 and 17 mm) and *F. avenaceum* (17, 17, and 18 mm). The antimicrobial analysis shows that the PEG-coated GO-NPs are suitable for antimicrobial activity.

4. Conclusion

The hummer's method was used to synthesize pure and coated GO-NPs for antimicrobial activity. The hexagonal lattice structureand crystallite size in the range of 7–16 nm were investigated with the help of XRD analysis. The irregular, non-uniform, rod shape, the spongy and randomly crumpled-like surface of graphite powder, pure, CA-coated, and PEG-coated GO-NPswere identified via SEM analysis. Moreover, the optical absorbance in the range of the UV region and the band gap decrease (2.30–2.03 eV) with CA and PEG-coated GO-NPs were calculated with UV–VIS analysis. The presence of different bands on the surface of the spectrum was measured by Raman spectroscopy analysis. After that, the antimicrobial activity against *A. hydrophila*, *E. coli* and *F. avenaceum* were done by using 10 and 20 mg/mL of pure and (PEG and CA) coated GO-NPs. The PEG-coated GO-NPs enhance the antimicrobial activity upto a significant level of inhibition zone of 20 mm. In future the polymer-coated GO-NPs are preferred for antioxidant and wound healing purposes.

Acknowledgement

Researchers Supporting Project number (RSP-2021/397), King Saud University, Riyadh, Saudi Arabia.

References

Ahmad, I., Malak, H.A., Abulreesh, H.H., 2021. Environmental antimicrobial resistance and its drivers: A potential threat to public health. J. Glob. Antimicrob. Resist. 27, 101–111.

Al Mogbel, M.S., Elabbasy, M.T., Mohamed, R.S., Ghoniem, A.E., Abd El-Kader, M.F.H., Menazea, A.A., 2021. Improvement in antibacterial activity of Poly Vinyl Pyrrolidone/Chitosan incorporated by graphene oxide NPs via laser ablation. J. Polym. Res. 28 (12), 1–8.

Bhargava, R., Khan, S., 2018. Structural, optical and dielectric properties of graphene oxide. In: AIP Conference Proceedings, vol. 1953, no. 1, AIP Publishing LLC, p. 030011.

Bilal, M.H., Mehmood, R., Fakhar-e-Alam, M., Munir, T., Saadullah, M., Mahmood, A., Mehmood-Ur-Rehman, K., 2021. Biocompatible graphene oxide (GO) nanobiosensor used for quantitative analysis of glucose. Digest J. Nanomater. Biostruct. (DJNB) 16 (1).

Chowdhury, I., Duch, M.C., Mansukhani, N.D., Hersam, M.C., Bouchard, D., 2014. Interactions of graphene oxide nanomaterials with natural organic matter and metal oxide surfaces. Environ. Sci. Technol. 48 (16), 9382–9390.

Chung, C., Kim, Y.K., Shin, D., Ryoo, S.R., Hong, B.H., Min, D.H., 2013. Biomedical applications of graphene and graphene oxide. Acc. Chem. Res. 46 (10), 2211–2224.

Georgieva, M., Gospodinova, Z., Keremidarska-Markova, M., Kamenska, T., Gencheva, G., Krasteva, N., 2021. PEGylated Nanographene Oxide in Combination with Near-Infrared Laser Irradiation as a Smart Nanocarrier in Colon Cancer Targeted Therapy. Pharmaceutics 13 (3), 424.

Hayes, W.I., Joseph, P., Mughal, M.Z., Papakonstantinou, P., 2015. Production of reduced graphene oxide via hydrothermal reduction in an aqueous sulphuric acid suspension and its electrochemical behaviour. J. Solid State Electrochem. 19 (2), 361–380.

Gospodinova, Z., Kamenska, T., Gencheva, G., Georgieva, M., Krasteva, N., 2021. PEGylation of graphene oxide nanosheets modulate cancer cell motility and proliferative ability. In: Journal of Physics: Conference Series, vol. 1762, no. 1. IOP Publishing, p. 012001.

Jabbar, A., Yasin, G., Khan, W.Q., Anwar, M.Y., Korai, R.M., Nizam, M.N., Muhyodin, G., 2017. Electrochemical deposition of nickel graphene composite coatings: effect of deposition temperature on its surface morphology and corrosion resistance. RSC Adv. 7 (49), 31100–31109.

Jihad, M.A., Noori, F., Jabir, M.S., Albukhaty, S., AlMalki, F.A., Alyamani, A.A., 2021. Polyethylene Glycol Functionalized Graphene Oxide Nanoparticles Loaded with Nigella sativa Extract: A Smart Antibacterial Therapeutic Drug Delivery System. Molecules 26 (11), 3067.

Johra, F.T., Lee, J.W., Jung, W.G., 2014. Facile and safe graphene preparation on solution based platform. J. Ind. Eng. Chem. 20 (5), 2883–2887.

Kamenska, T., Abrashev, M., Georgieva, M., Krasteva, N., 2021. Impact of Polyethylene Glycol Functionalization of Graphene Oxide on Anticoagulation and Haemolytic Properties of Human Blood. Materials 14 (17), 4853.

Li, Z., Jiang, S., Huo, Y., Ning, T., Liu, A., Zhang, C., Man, B., 2018. 3D silver nanoparticles with multilayer graphene oxide as a spacer for surface enhanced Raman spectroscopy analysis. Nanoscale 10 (13), 5897–5905.

Muhammad, M.H., Idris, A.L., Fan, X., Guo, Y., Yu, Y., Jin, X., Huang, T., 2020. Beyond risk: bacterial biofilms and their regulating approaches. Front. Microbiol. 11, 928.

Munir, T., Latif, M., Mahmood, A., Malik, A., Shafiq, F., 2020. Influence of IP-injected ZnO-nanoparticles in Catlacatla fish: hematological and serological profile. Naunyn-Schmiedeberg's Arch. Pharmacol. 393 (12), 2453–2461.

Munir, T., Mahmood, A., Shafiq, F., Fakhar-e-Alam, M., Atif, M., Raza, A., Abbas, N., 2021. Experimental and theoretical analyses of nano-silver for antibacterial activity based on differential crystal growth temperatures. Saudi J. Biol. Sci. 28 (12), 7561–7566.

Olborska, A., Janas-Naze, A., Kaczmarek, Ł., Warga, T., Halin, D.S. C., 2020. Antibacterial Effect of Graphene and Graphene Oxide as a Potential Material for Fiber Finishes. Autex Res. J. 1 (ahead-of-print).

Orth, E.S., Fonsaca, J.E., Domingues, S.H., Mehl, H., Oliveira, M.M., Zarbin, A.J., 2013. Targeted thiolation of graphene oxide and its utilization as precursor for graphene/silver nanoparticles composites. Carbon 61, 543–550.

Plachá, D., Jampilek, J., 2019. Graphenic materials for biomedical applications. Nanomaterials 9 (12), 1758.

Priyadarsini, S., Mohanty, S., Mukherjee, S., Basu, S., Mishra, M., 2018. Graphene and graphene oxide as nanomaterials for medicine and biology application. J. Nanostruct. Chem. 8 (2), 123–137.

Robkhob, P., Ghosh, S., Bellare, J., Jamdade, D., Tang, I.M., Thongmee, S., 2020. Effect of silver doping on antidiabetic and antioxidant potential of ZnO nanorods. J. Trace Elem. Med. Biol. 58, 126448.

Samadian, H., Mohammad-Rezaei, R., Jahanban-Esfahlan, R., Massoumi, B., Abbasian, M., Jafarizad, A., Jaymand, M., 2020. A de novo theranostic nanomedicine composed of PEGylated graphene oxide and gold nanoparticles for cancer therapy. J. Mater. Res. 35 (4), 430–441.

Sengupta, I., Bhattacharya, P., Talukdar, M., Neogi, S., Pal, S.K., Chakraborty, S., 2019. Bactericidal effect of graphene oxide and reduced graphene oxide: Influence of shape of bacteria. Colloid Interface Sci. Commun. 28, 60–68.

Sunderrajan, S., Miranda, L.R., Pennathur, G., 2018. Improved stability and catalytic activity of graphene oxide/chitosan hybrid beads loaded with porcine liver esterase. Prep. Biochem. Biotech. 48 (4), 343–351.

Usman, M.S., Hussein, M.Z., Kura, A.U., Fakurazi, S., Masarudin, M.J., Ahmad Saad, F.F., 2018. Graphene oxide as a nanocarrier for a theranostics delivery system of protocatechuic acid and gadolinium/gold nanoparticles. Molecules 23 (2), 500.

Valentini, F., Calcaterra, A., Ruggiero, V., Pichichero, E., Martino, A., Iosi, F., Mari, E., 2019. Functionalized graphene derivatives: Antibacterial properties and cytotoxicity. J. Nanomater.